

**Benchmarking ionomers for CO<sub>2</sub> electroreduction to multicarbon products in zero-gap electrolyzers**

Fan Zeng<sup>1,2</sup>, Huiying Deng<sup>1,2</sup>, Mengjiao Zhuansun<sup>1,2</sup>, Wenzhi Teng<sup>1,2</sup>, and Yuhang Wang<sup>1,2,\*</sup>

<sup>1</sup>Institute of Functional Nano & Soft Materials (FUNSOM), Soochow University, Suzhou, Jiangsu, 215123, China.

<sup>2</sup>Jiangsu Key Laboratory for Advanced Negative Carbon Technologies, Soochow University, Suzhou, Jiangsu, 215123, China.

## **Experimental Procedures**

### **Electrode Preparation**

Cathode preparation: Cathodes were prepared by sputtering 200 nm of Cu (99.99%) onto a porous PTFE membrane (0.4  $\mu\text{m}$  pores) using a magnetron sputtering instrument (Nanjing Tansi Technology Co., Ltd). Ionomers were dispersed in an appropriate amount of isopropanol (Sinopharm-Shanghai Test) and sonicated until a uniform dispersion was formed, and then sprayed onto the surface of Cu-PTFE.

The ionomers included Pention D18, D35, D72 (5 wt% in isopropanol, Xergy Co., Ltd.), Sustainion XA-9, PiperION A5, Aquivion PW87S, Nafion (5 wt%, Sigma Aldrich), and QAPPT (5 wt%, EVE Hydrogen Energy Co., Ltd).

Anode preparation: The anode was prepared by depositing  $\text{IrO}_2$  on titanium mesh supports through infiltration and thermal decomposition methods. Briefly, the titanium mesh was degreased with propanol and deionised water, and then immersed in 6 M hydrochloric acid at 90  $^\circ\text{C}$  for 50 minutes for etching. A solution containing 300 mg  $\text{IrCl}_3 \cdot x\text{H}_2\text{O}$  (50-58%, J&K), 16 mL hydrochloric acid (AR, Yonghua), and 40 mL isopropanol (Sinopharm-Shanghai Test) was prepared. Subsequently, the etched titanium mesh was immersed in the  $\text{IrCl}_3$  solution for 5-10 minutes, dried in an oven, and then calcined in a furnace at 500  $^\circ\text{C}$  for 10 minutes.

### **Assembly of MEA:**

A  $2.5 \times 2.5 \text{ cm}^2$  ionomer-coated Cu-PTFE electrode was prepared as the cathode, and a titanium mesh supported  $\text{IrO}_2$  was used as the anode. To enhance electronic conductivity, the edge of the cathode was covered and secured onto the flow field using copper tapes. These copper tapes were then covered with Kapton tapes to prevent corrosion and potential interference with the reaction. A  $3 \times 3 \text{ cm}^2$  anion exchange membrane (Sustainion X37-50, grade 60) was placed on the cathode, and the  $2.5 \times 2.5 \text{ cm}^2$  anode was stacked on top of the ion exchange membrane, aligned with the cathode. The cathode and anode plates were then tightly screwed together to prevent liquid and gas leakage.

### **Material Characterisations**

SEM images were captured using a Zeiss G500 scanning electron microscope. Fourier transform infrared spectroscopy (FTIR) was conducted on the samples using a Nicolet iS-50 infrared spectrometer with a scanning range of 400~4000  $\text{cm}^{-1}$ . The contact angle image was obtained from DataPhysics OCA.

### **Electrochemical measurements**

Carbon dioxide reduction reaction ( $\text{CO}_2\text{RR}$ ): The  $\text{CO}_2\text{RR}$  was performed in a zero-gap membrane electrode assembly (MEA) electrolyser (5  $\text{cm}^2$ , DioxideMaterials Corporation). Humidified  $\text{CO}_2$  gas continuously enters the cathode side at a flow rate of 30 sccm through a digital mass flow controller (CS200 A, from Sevenstar Flow (Beijing) Co., Ltd). The 0.1 M  $\text{KHCO}_3$  ( $\geq 99\%$ , Aldrich) electrolyte is pumped into the anode side by a peristaltic pump at a speed of 60  $\text{ml min}^{-1}$ , and an anion exchange membrane (Sustainion X37-50, grade 60) is placed between the anode and cathode electrodes. Electrochemical measurements were conducted using a DH7002 potentiostat (from Donghua Analytical Instruments (Taizhou) Co., Ltd). Chronopotentiometry ( $V \sim t$ ) measurements were carried out at current densities ranging from 20  $\text{mA cm}^{-2}$  to 220  $\text{mA cm}^{-2}$ . Gas products were

analysed with a gas chromatograph equipped with a thermal conductivity detector (TCD) and a flame ionisation detector (FID). Liquid products were analysed using high-performance liquid chromatography (HPLC, Vanquish Core, ThermoFisher). The gas and liquid products were calibrated using the external standard method.

Oxygen evolution reaction (OER): The OER was performed in the aforementioned MEA electrolyser. In contrast to the CO<sub>2</sub>RR setup, the positive and negative electrodes are reversed. A sealed device with an Ag/AgCl reference electrode connected outside the anode forms a three-electrode system. Chronopotentiometry (V~t) measurements were conducted at current densities ranging from 20 mA cm<sup>-2</sup> to 220 mA cm<sup>-2</sup> using the DH7002 potentiostat.

#### Faradaic efficiency (FE) calculations:

The Faraday efficiency (FE) of gaseous products was calculated using the following equation:

$$FE = \frac{F \times n \times V_{gas} \times c}{i \times V_m} \#(1)$$

Where  $F$  represents the Faraday constant,  $n$  represents the number of electron transfers required to produce 1 mol of gas product,  $V_{gas}$  represents the flow rate of supplied CO<sub>2</sub>,  $c$  represents the detected gas product concentration,  $i$  represents the total operating current, and  $V_m$  represents the unit molar volume of gas at 298.15 K (24.5 L mol<sup>-1</sup>).

The FE for the liquid product is calculated according to the following equation:

$$FE = m_i \times \frac{F \times n}{i \times t} \#(2)$$

Where  $m_i$  is the mole of liquid products, and  $t$  is the duration of the measured product.

#### Tafel Slope calculations:

In electrochemical experiments, the kinetic relationship is usually represented by the Butler-Volmer equation:

$$j = j_0 \left[ \exp\left(\frac{\alpha_a n F E}{RT}\right) + \exp\left(-\frac{\alpha_c n F E}{RT}\right) \right] \#(3)$$

Where  $j$  is the current density,  $j_0$  is the exchange current density,  $\alpha_a$  is the anode electron transfer coefficient,  $\alpha_c$  is the cathode electron transfer coefficient,  $n$  is the number of transferred electrons in the reaction,  $F$  is the Faraday constant,  $E$  is the applied voltage,  $R$  is the gas constant, and  $T$  is the thermodynamic temperature.

Simplified (3) to obtain the Tafel equation:

$$j = j_0 \exp\left(\frac{\alpha_a n F E \eta}{RT}\right) \#(4)$$

Where  $\eta$  is overpotential.

Take the logarithm of (4) on both sides to obtain the Tafel curve:

$$\lg(j_x) = \lg(j_0) + \frac{\eta}{b} \#(5)$$

Where  $b$  is the Tafel slope, and  $j_x$  is the partial current density of  $x$  product ( $x$  is the product of carbon dioxide reduction reaction).

Overpotential  $\eta$  calculation:

The CO<sub>2</sub>RR test of MAE can obtain the voltage  $E_{cell}$  of the entire battery reaction, while the OER test of the three-electrode system can obtain the voltage  $E_{OER}(Ag/AgCl)$  of the anode reaction relative to the Ag/AgCl reference. The voltage  $E_{CO_2RR}(Ag/AgCl)$  of CO<sub>2</sub>RR relative to Ag/AgCl can be obtained from Equation(6):

$$E_{CO_2RR}(Ag/AgCl) = E_{cell} - E_{OER}(Ag/AgCl) \#(6)$$

The potential of CO<sub>2</sub>RR relative to the reversible hydrogen electrode  $E_{CO_2RR}(RHE)$  is calculated by the following equation:

$$E_{CO_2RR}(RHE) = E_{CO_2RR}(Ag/AgCl) + 0.059 \times pH + 0.197 \#(7)$$

Overpotential  $\eta$  is calculated from the following equation:

$$\eta = E_{CO_2RR}(RHE) + E_0 \#(8)$$

Where  $E_0$  is the standard equilibrium potential of each product in the carbon dioxide reduction reaction.

### **Operando Raman spectra measurements:**

Operando Raman spectra measurements were performed in a flow cell with a platinum wire as the counter electrode (CE) and Ag/AgCl as the reference electrode (RE). Due to the extremely poor conductivity of the PTFE substrate in the flow cell, the working electrode was fabricated by using electrodes composed of copper powder thoroughly mixed with the ionomers, which were then sprayed onto carbon paper (MB30). The ionomers (D18, Nafion, Sustainion, PiperION, and D72) served as modulators of hydrophilicity on the catalyst surface, consistent with their role on the PTFE substrate. During the measurement, a water immersion objective was positioned approximately 1 mm from the electrode surface. The laser used had a wavelength of 633 nm with a scanning range of 300-3400 cm<sup>-1</sup>. The voltage range of the tested CO<sub>2</sub>RR was -1.1 to -2.5 V vs. Ag/AgCl, the exposure time was 20 s, the laser power was set at 10%, and the integration time was 4 s.

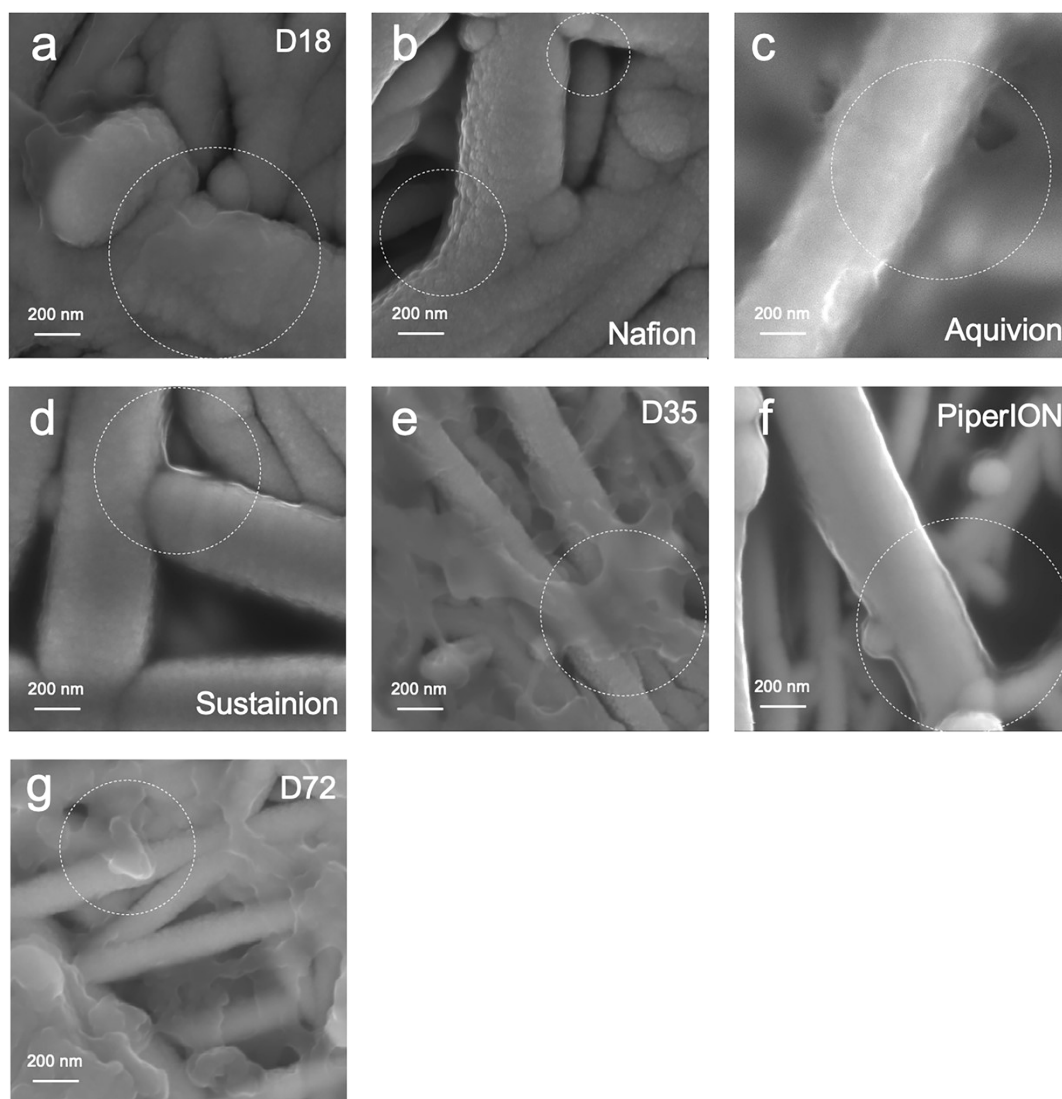


**Figure S1.** SEM images of (a), D18 (b) Nafion, (c) Aquivion, (d) Sustainion, (e) D35, (f) PiperION, and (g) D72 on Cu-PTFE. The ionomer on the Cu-PTFE catalyst is indicated using dotted lines.

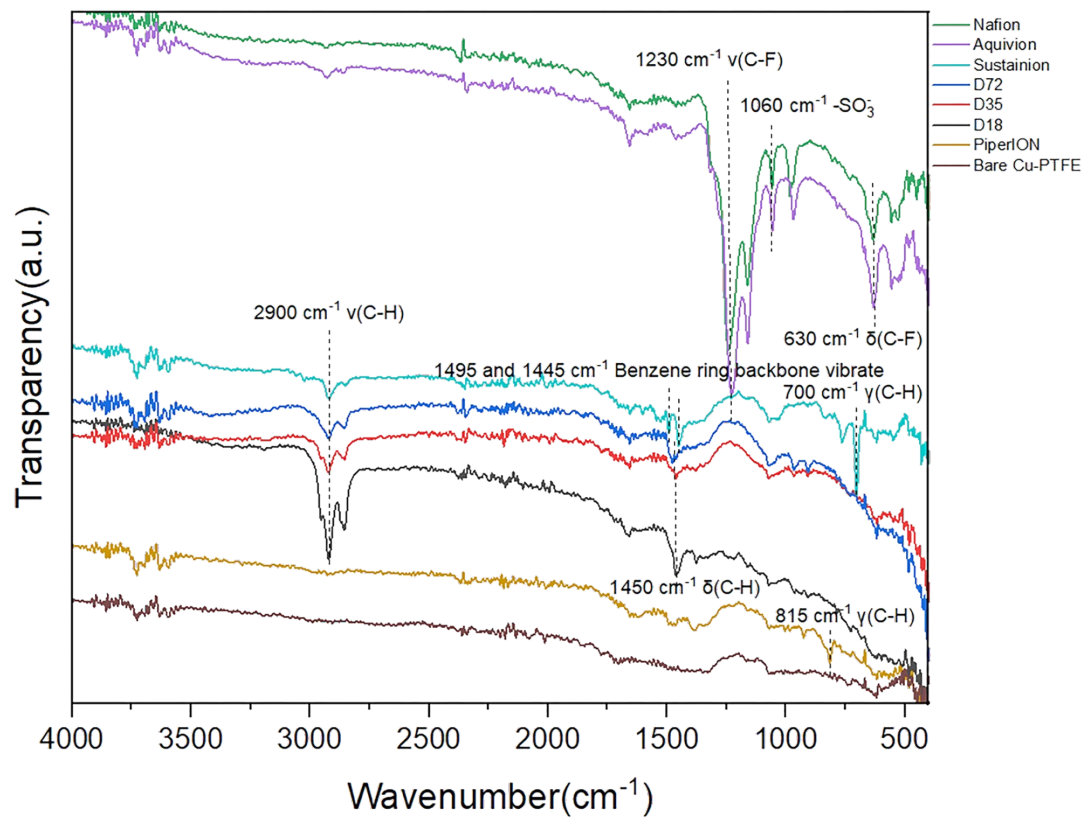


**Figure S2.** FTIR spectra of ionomers on Cu-PTFE.

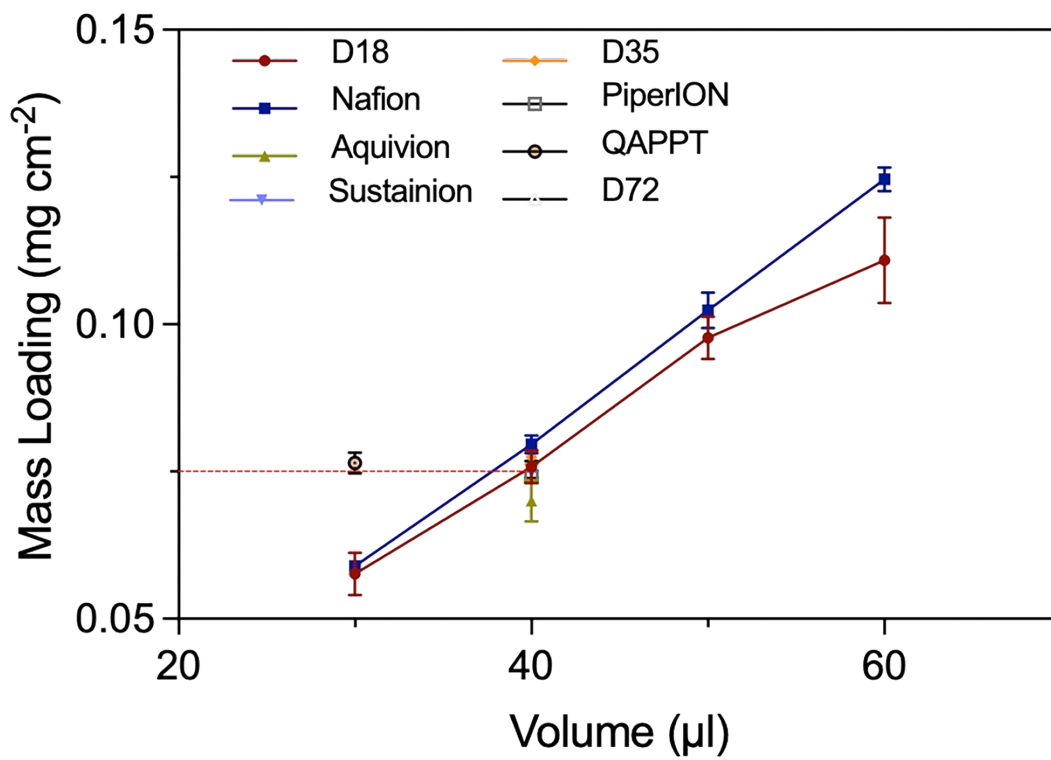


**Figure S3.** The mass loading of 30 μl, 40 μl, 50 μl and 60 μl D18 and Nafion on Cu-PTFE, and that of 40 μl Aquivion, Sustainion, D35, PiperION, QAPPT, and D72, respectively.

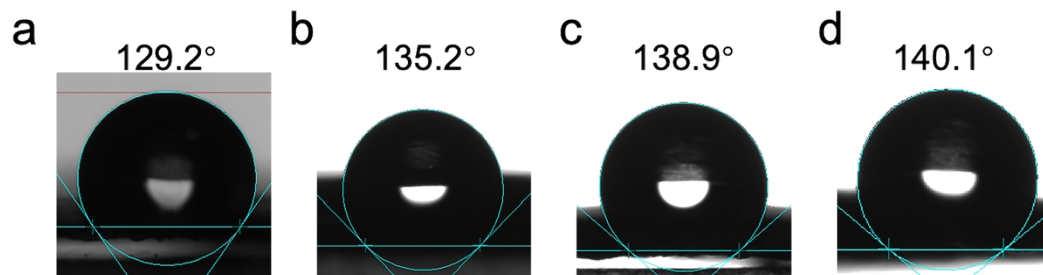


**Figure S4.** Contact angles between water drops and Cu-PTFE coated with (a) 30  $\mu\text{l}$ , (b) 40  $\mu\text{l}$ , (c) 50  $\mu\text{l}$ , and (d) 60  $\mu\text{l}$  D18.



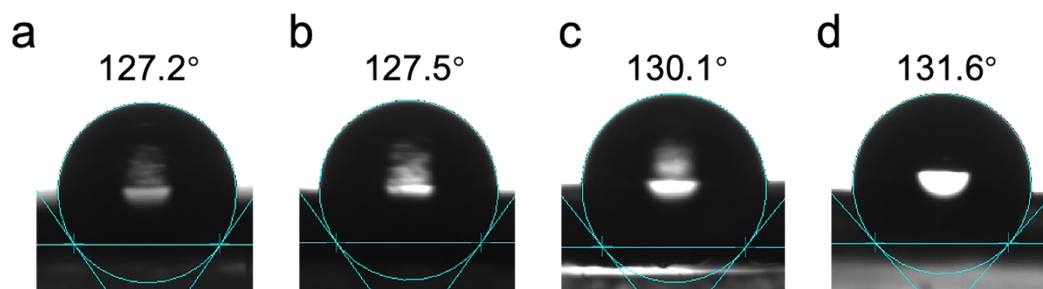


**Figure S5.** Contact angles between water drops and Cu-PTFE coated with (a) 30  $\mu\text{l}$ , (b) 40  $\mu\text{l}$ , (c) 50  $\mu\text{l}$ , and (d) 60  $\mu\text{l}$  Nafion.

98.3°

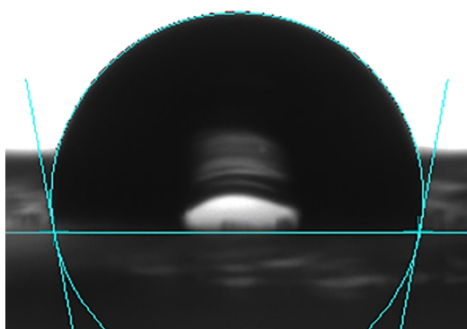


**Figure S6.** Contact angle between a water drop and bare Cu-PTFE.

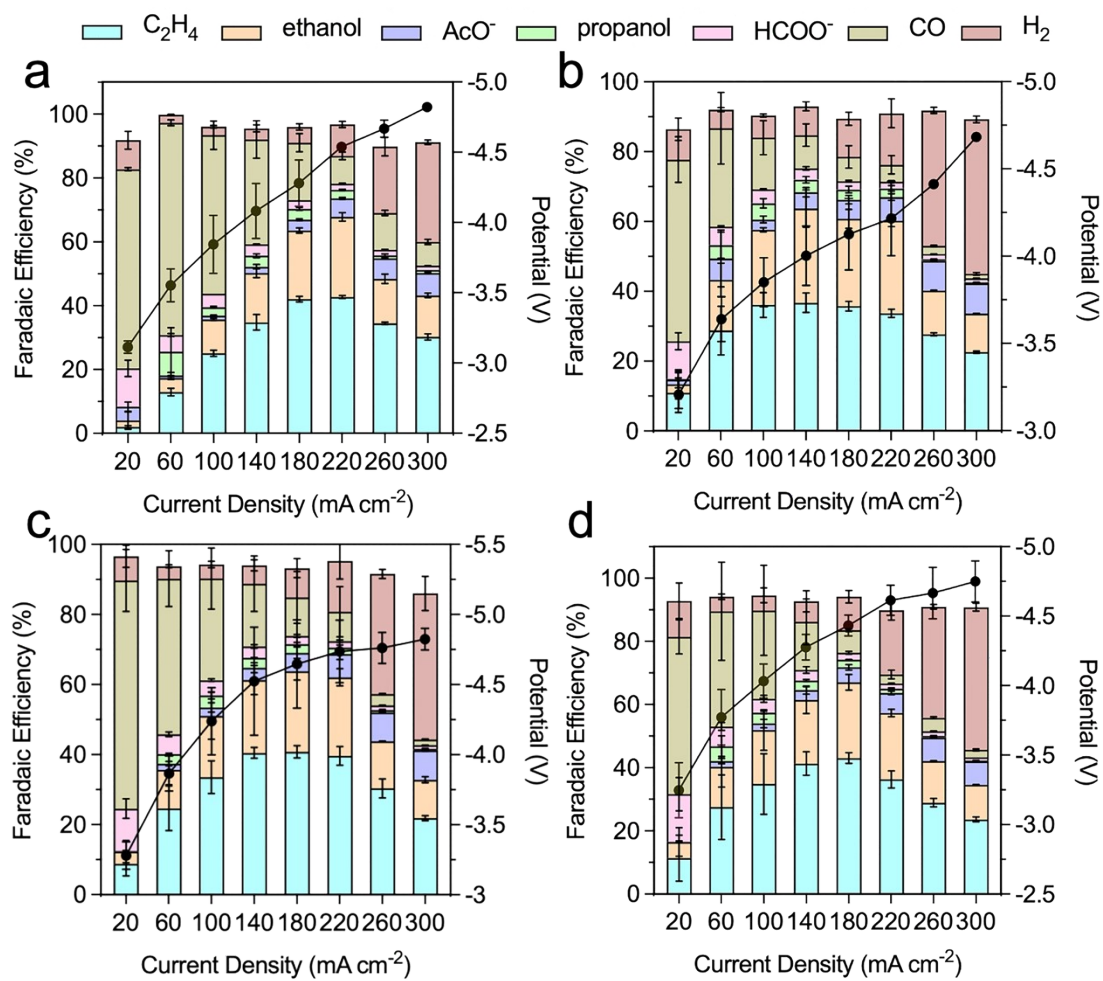


**Figure S7.** Product FEs on Cu-PTFE coated with (a) 30  $\mu\text{l}$ , (b) 40  $\mu\text{l}$ , (c) 50  $\mu\text{l}$ , and (d) 60  $\mu\text{l}$  D18. Error bars correspond to the standard deviation of three independent measurements.

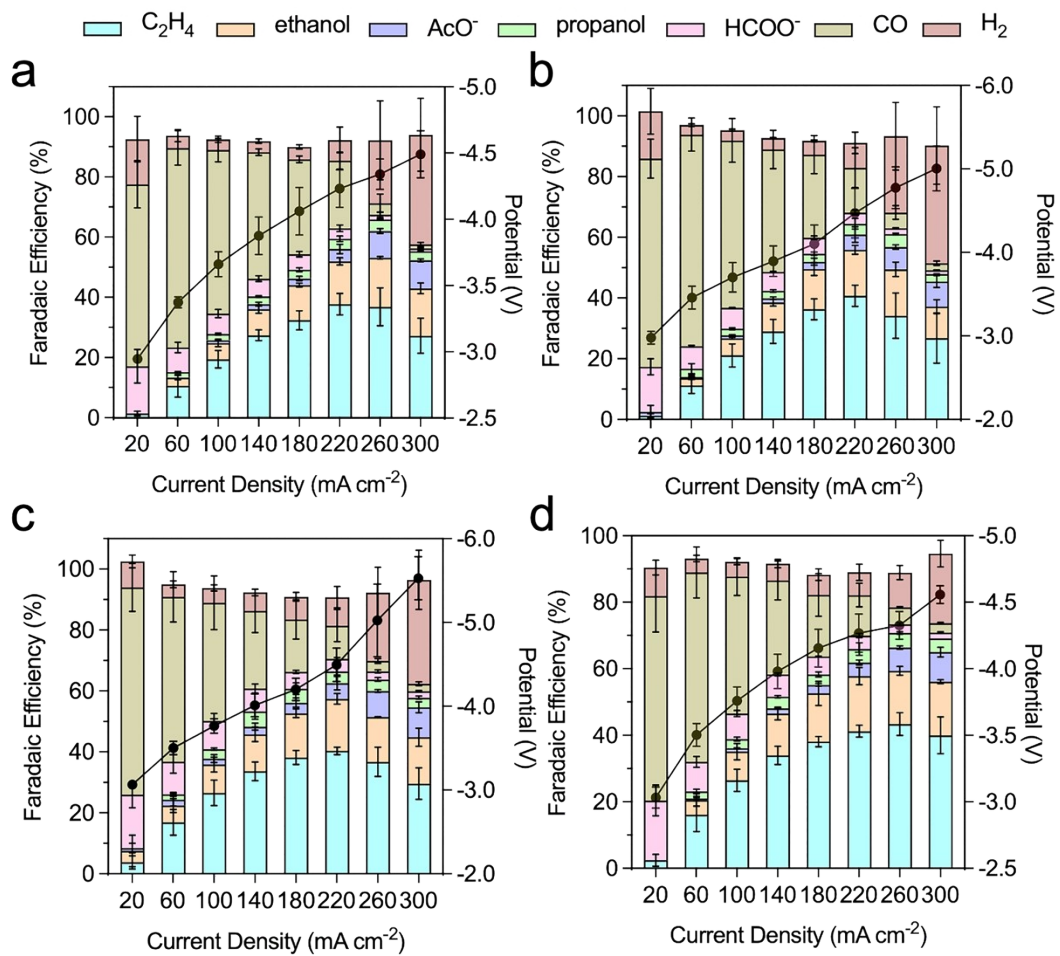


**Figure S8.** Product FEs on Cu-PTFE coated with (a) 30 μl, (b) 40 μl, (c) 50 μl, and (d) 60 μl Nafion. Error bars correspond to the standard deviation of three independent measurements.

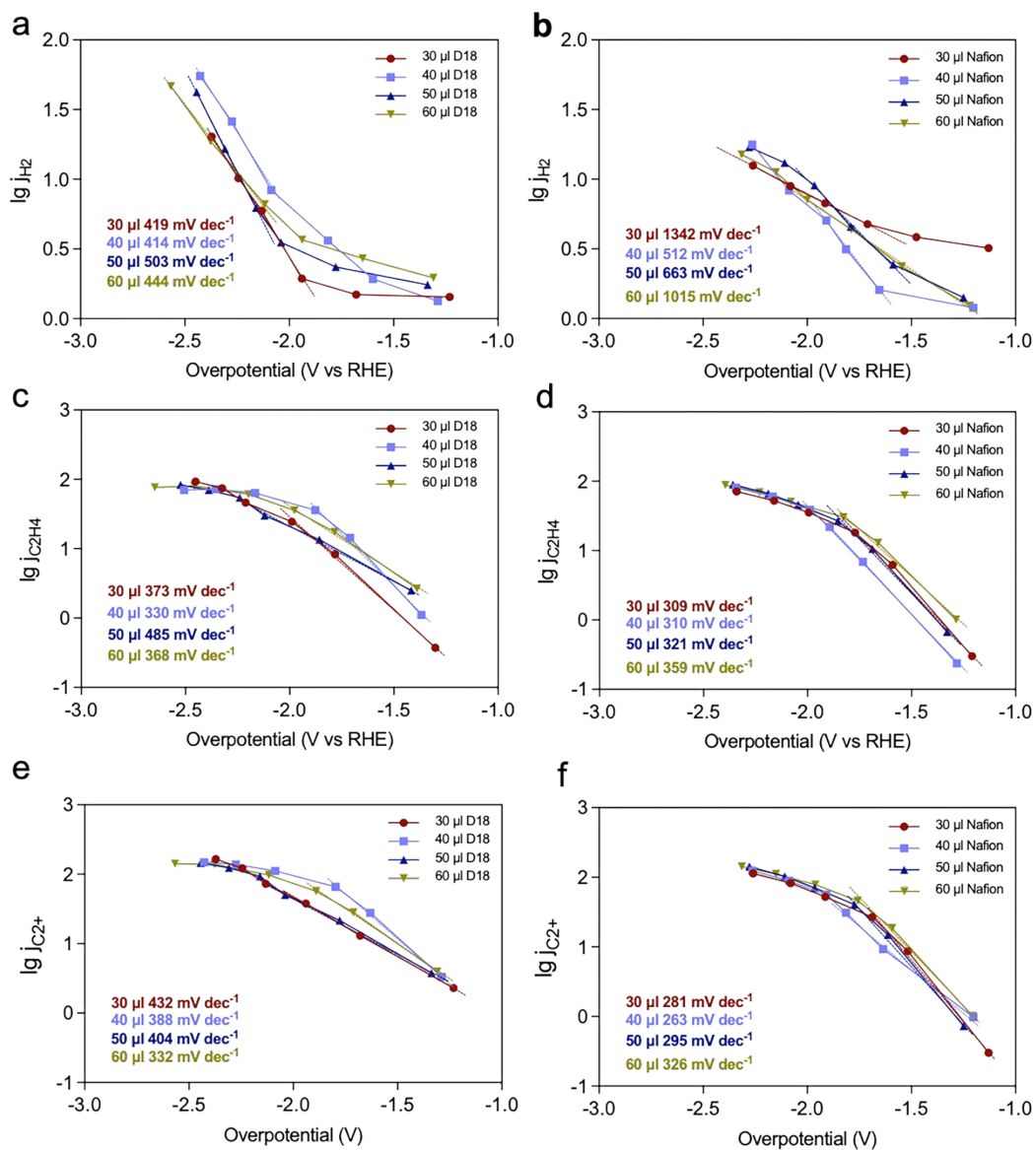


**Figure S9.** Tafel analysis for (a-b)  $H_2$  production on D18 and Nafion Cu-PTFE catalyst, (c-d)  $C_2H_4$  production on D18 and Nafion Cu-PTFE catalyst, and (e-f)  $C_{2+}$  production on D18- and Nafion-Cu.

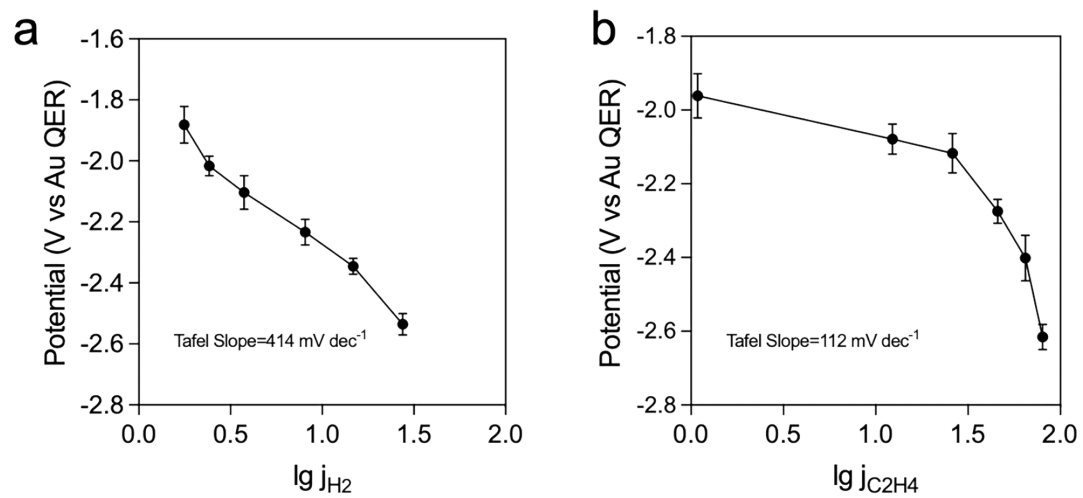


**Figure S10.** Tafel analysis for (a) H<sub>2</sub> and (b) C<sub>2</sub>H<sub>4</sub> on 40  $\mu$ l D18 Cu-PTFE catalyst under pure water conditions. Error bars correspond to the standard deviation of two independent measurements.

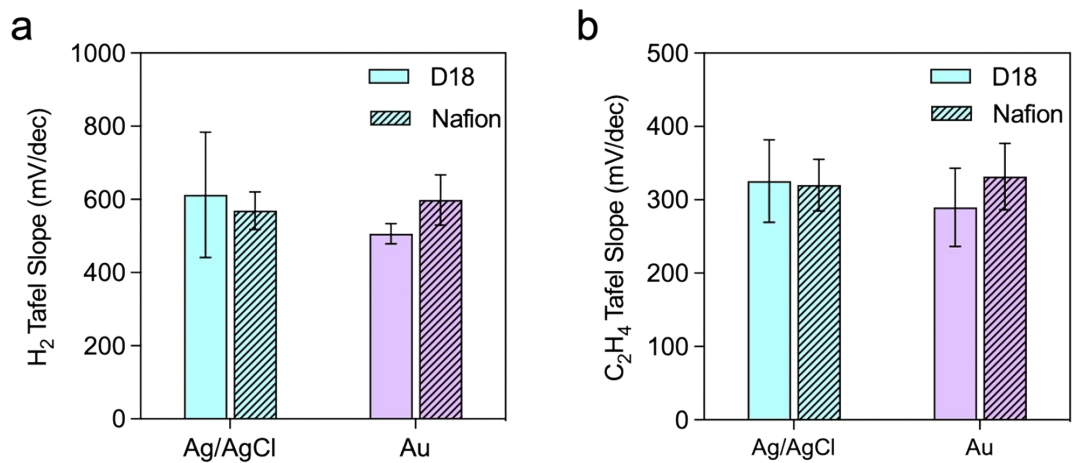


**Figure S11.** Comparison of Tafel analysis for (a) H<sub>2</sub> and (b) C<sub>2</sub>H<sub>4</sub> between systems with Ag/AgCl as a reference and systems with Au as a reference. Error bars correspond to the standard deviation of three independent measurements.

**a**

	content/ $\mu\text{l}$	Tafel Slope/ $\text{mV}\cdot\text{dec}^{-1}$	$j_{\text{max}}/\text{mA}\cdot\text{cm}^{-2}$
D18	30	419	20
	40	414	42
	50	503	33
	60	444	50

**b**

	content/ $\mu\text{l}$	Tafel Slope/ $\text{mV}\cdot\text{dec}^{-1}$	$j_{\text{max}}/\text{mA}\cdot\text{cm}^{-2}$
D18	30	373	93
	40	330	76
	50	485	94
	60	368	87

**c**

	content/ $\mu\text{l}$	Tafel Slope/ $\text{mV}\cdot\text{dec}^{-1}$	$j_{\text{max}}/\text{mA}\cdot\text{cm}^{-2}$
D18	30	432	166
	40	388	157
	50	404	161
	60	332	149

**Table S1.** The Tafel analysis result for (a)  $\text{H}_2$ , (b)  $\text{C}_2\text{H}_4$ , and (c)  $\text{C}_{2+}$  products of D18-Cu.



**a**

	content/ $\mu\text{l}$	Tafel Slope/ $\text{mV}\cdot\text{dec}^{-1}$	$j_{\text{max}}/\text{mA}\cdot\text{cm}^{-2}$
Nafion	30	1342	30
	40	512	30
	50	663	32
	60	1015	31

**b**

	content/ $\mu\text{l}$	Tafel Slope/ $\text{mV}\cdot\text{dec}^{-1}$	$j_{\text{max}}/\text{mA}\cdot\text{cm}^{-2}$
Nafion	30	309	84
	40	310	82
	50	321	90
	60	359	108

**c**

	content/ $\mu\text{l}$	Tafel Slope/ $\text{mV}\cdot\text{dec}^{-1}$	$j_{\text{max}}/\text{mA}\cdot\text{cm}^{-2}$
Nafion	30	281	157
	40	263	148
	50	295	173
	60	326	174

**Table S2.** The Tafel analysis result for (a)  $\text{H}_2$ , (b)  $\text{C}_2\text{H}_4$ , and (c)  $\text{C}_{2+}$  products of Nafion-Cu.

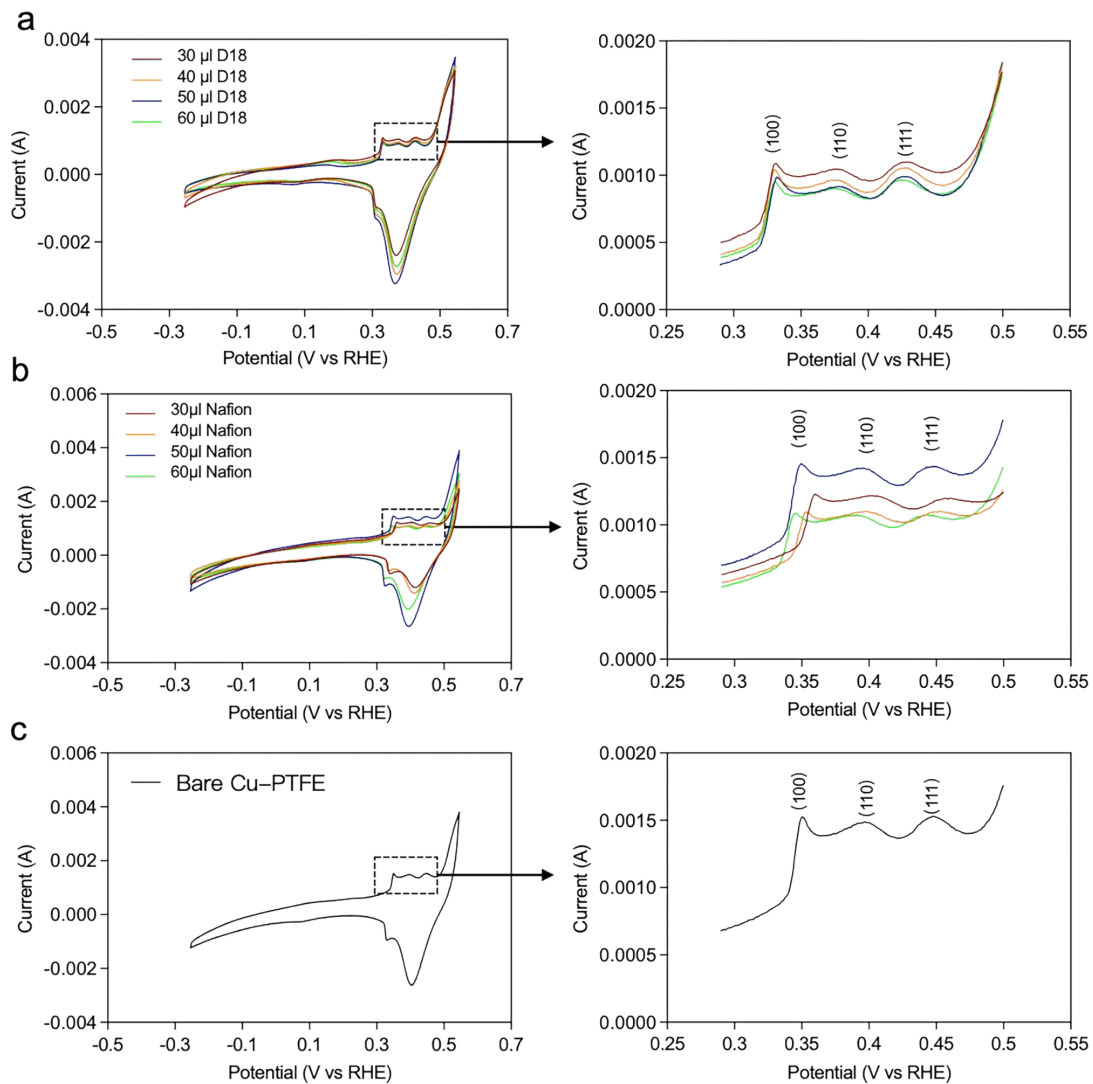


**Figure S12.** Linear sweep voltammetry profiles of (a) D18 (b) Nafion (c) Bare Cu-PTFE. The oxidation peaks correspond to the electrochemical OH<sup>-</sup> adsorption waves on Cu (100), Cu (110) and Cu (111) planes.

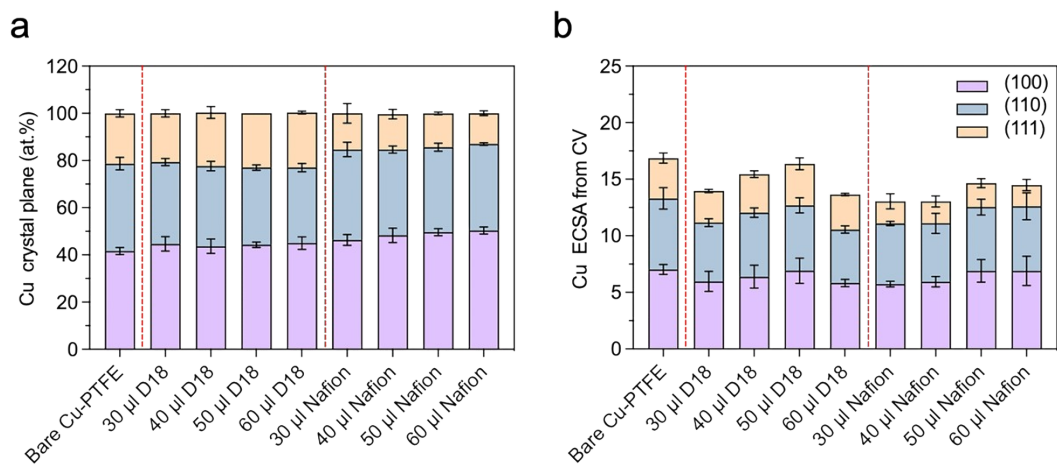


**Figure S13.** (a) The proportion of the three crystal planes of copper to the total crystal plane. (b) The ECSA of each facet. The ECSA is obtained by integrating the oxidation peak and dividing it by the ECSA of copper foil with the same geometric area.

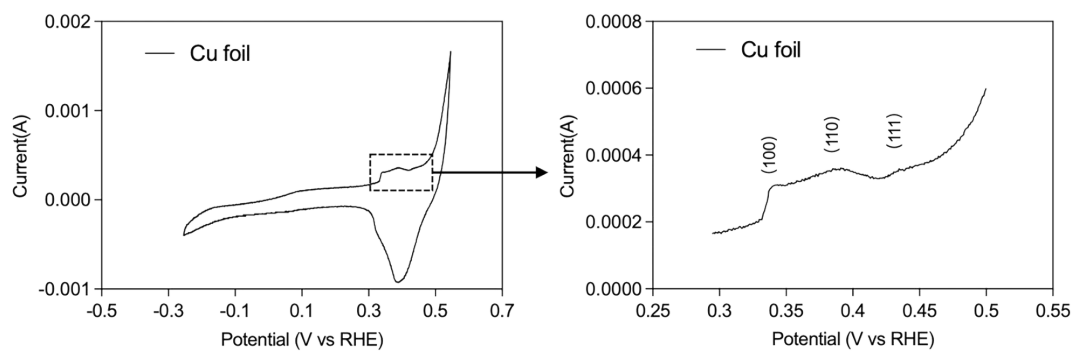


**Figure S14.** Linear sweep voltammetry profiles of electropolished Cu foil. The oxidation peaks correspond to the electrochemical  $\text{OH}^-$  adsorption waves on Cu (100), Cu (110), and Cu (111) planes.

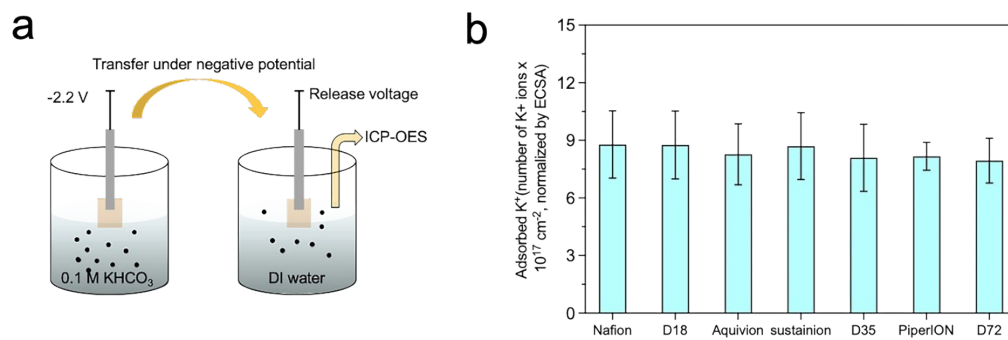


**Figure S15.** Comparison of  $\text{K}^+$  adsorption capacities of all ionomers. (a) The methodology for  $\text{K}^+$  retention measurements. (b) ECSA-normalized adsorbed  $\text{K}^+$  numbers on Nafion-, D18-, Aquivion-, Sustainion-, D35-, PiperION-, and D72-Cu.

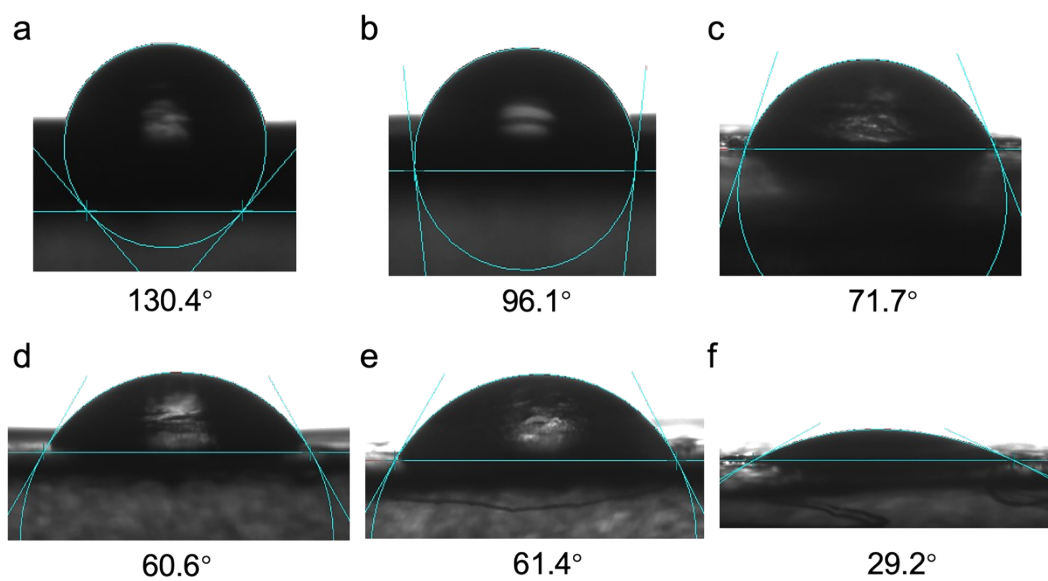


**Figure S16.** Contact angles of (a) Aquivion, (b) Sustainion, (c) D35, (d) PiperION, (e) QAPPT, and (f) D72 coated Cu-PTFE.

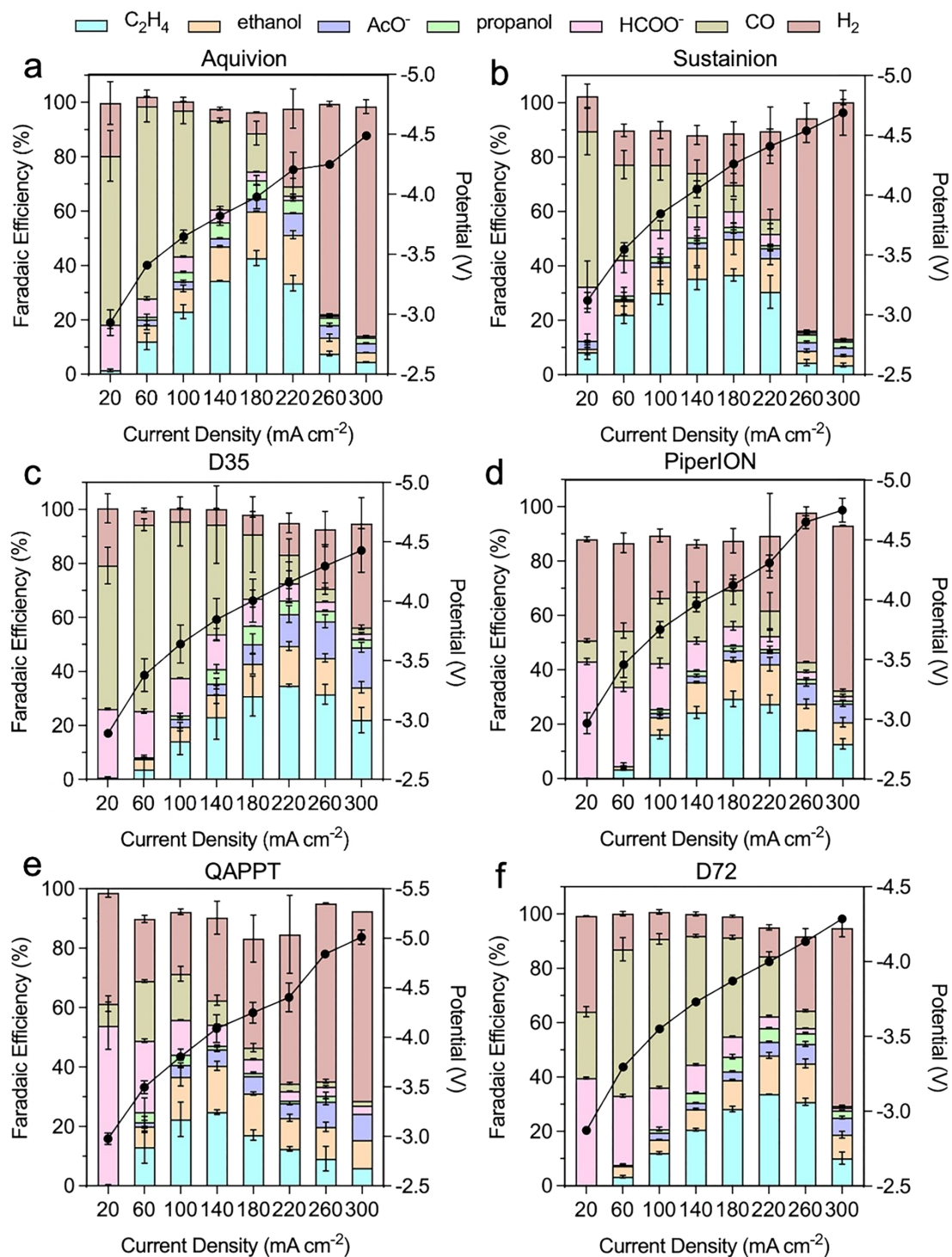


**Figure S17.** Product Faradaic efficiency of (a) Aquivion (b) Sustainion (c) D35 (d) PiperION (e) QAPPT (f) D72 coated Cu-PTFE catalyst. Error bars correspond to the standard deviation of three independent measurements.

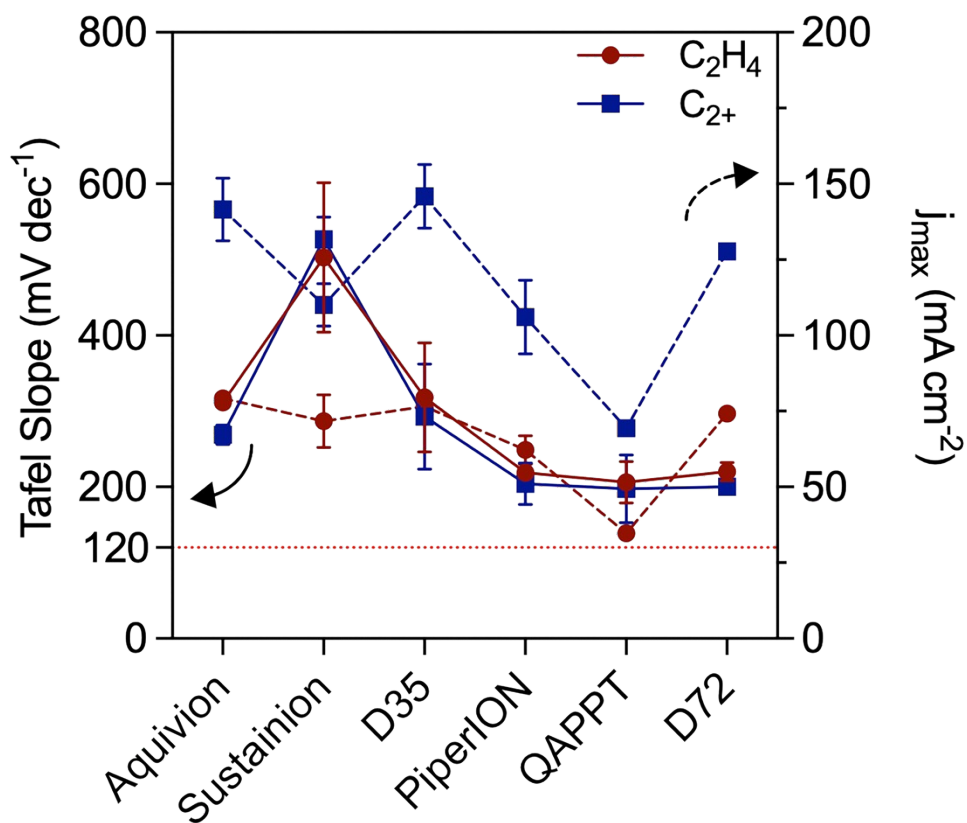


**Figure S18.** Tafel slopes (full line) and limiting diffusion currents (dotted line) for  $C_2H_4$  and  $C_2+$  production on Aquivion-, Sustainion-, D35-, PiperION-, QAPPT-, and D72-Cu. Error bars represent the standard deviations of at least three independent measurements.



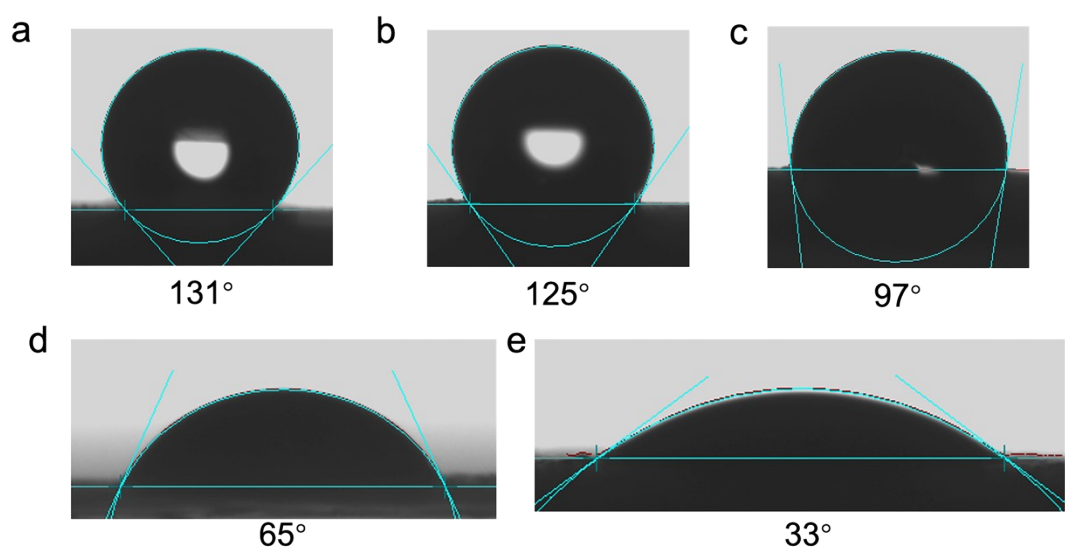


**Figure S19.** Contact angle of (a) D18 (b) Nafion (c) Sustainion (d) PiperION (e) D72 on the carbon paper.

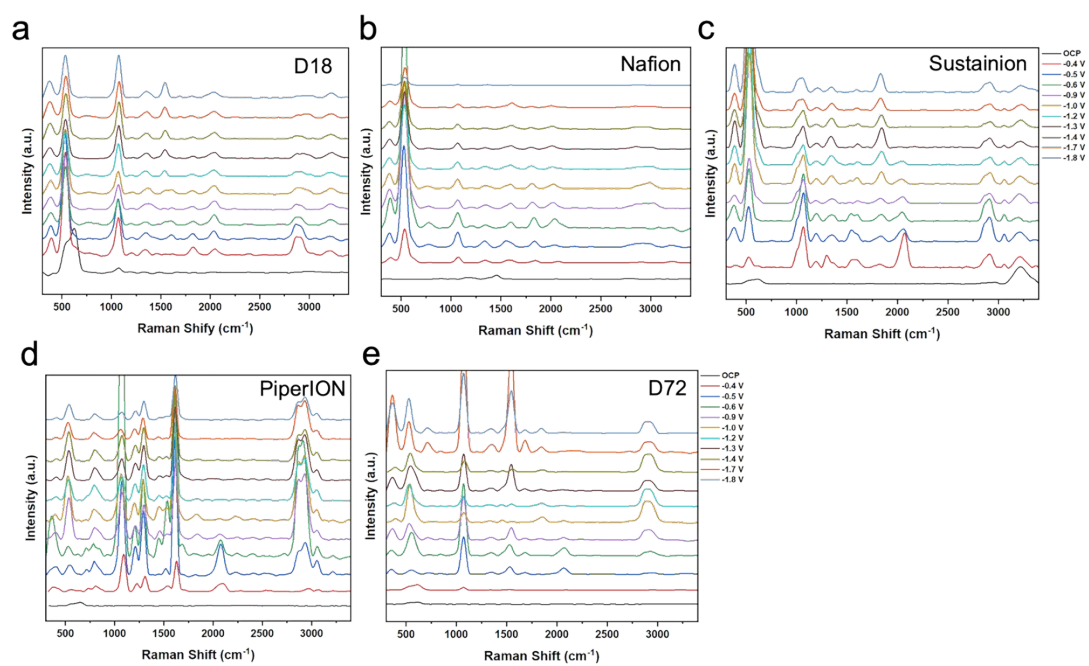


**Figure S20.** Additional in situ Raman spectra. The spectra were collected on (a) D18-Cu, (b) Nafion-Cu, (c) Sustainion-Cu, (d) PiperION-Cu, and (e) D72-Cu in a Raman Shift range of 300-3400 cm<sup>-1</sup>.